Available online at www.sciencedirect.com
SCIENCE DIRECT
Bioorganic & Medicinal Chemistry Letters
Bioorganic & Medicinal Chemistry Letters 16 (2006) 2580–2583

Human methionine aminopeptidase type 2 in complex with L- and D-methionine

M. Cristina Nonato, Joanne Widom and Jon Clardy*

Department of Chemistry and Chemical Biology, Baker Laboratory, Cornell University, Ithaca, NY 14853-1301, USA

Received 2 February 2006; accepted 16 February 2006
Available online 15 March 2006

Abstract—Human methionine aminopeptidase type 2 (hMetAP-2) was identified as the molecular target of anti-angiogenic agents such as fumagillin and its analogues. We describe here the crystal structure of hMetAP-2 in complex with L-methionine and D-methionine at 1.9 and 2.0 Å resolution, respectively. The comparison of the structure of the two complexes establishes the basis of enantiomer discrimination and provides some considerations for the design of selective MetAP-2 inhibitors.

Methionine aminopeptidase (MetAP) is a dimetalloprotease that catalyzes the removal of N-terminal methionine in newly formed polypeptide chains.[1,2] MetAPs are found in both eukaryotic and prokaryotic cells, and two types of MetAPs are recognized from amino acid sequence comparisons and structural studies: type 1 (MetAP-1) and type 2 (MetAP-2). MetAP activity is essential for survival, as the removal of N-terminal initiator methionines precedes post-translational modifications such as acetylation and myristoylation, which are required for proper localization and stability of proteins.[3] In prokaryotes, the deletion of the single MetAP gene is a lethal event.[4] In yeast, the deletion of either MetAP gene results in a slow growth phenotype, and deletion of both types is lethal.[5] While the detailed biological roles of various MetAPs remain to be defined, two independent papers have identified human methionine aminopeptidase type 2 (hMetAP-2) as the molecular target of the fungal metabolite fumagillin and its derivatives. These epoxide-containing natural products are potent anti-angiogenic compounds through irreversible covalent inhibition of hMetAP-2.[6–8]

Angiogenesis, the formation of new blood vessels, has been identified as an essential step in the growth and proliferation of cancer cells as well as a prominent feature in diabetic retinopathy, hemangiomas, arthritis, and psoriasis.[9–11]

Currently, TNP-470, a fumagillin synthetic derivative, is in clinical trials for cancer treatment. Although the ability of fumagillin and analogues to inhibit endothelial cell growth is related to their ability to inhibit MetAP-2 activity, it is not fully established why endothelial cell proliferation requires MetAP-2 activity. This study was undertaken to better understand the interactions in the binding pocket and active site of hMetAP-2 for the design of reversible and specific inhibitors.

Lowther et al. have described structural and biochemical studies on type 1 methionine aminopeptidase from *Escherichia coli*, eMetAP-1, and these studies have provided important insights into the structure-based design of inhibitors for this type 1 enzyme.[12] A particularly interesting example is their analysis of the crystal structure of eMetAP-1 in complex with the substrate-like inhibitor (3*R*)-amino-(2*S*)-hydroxyheptanoyl-L-Ala-L-Leu-L-Val-L-Phe-Ome, an analogue of the natural product bestatin.[12] Those results, besides clarifying possible reaction mechanisms for eMetAP-1, suggested that an unnatural absolute configuration at the Cα mimic of methionine—a D- not an L-amino acid—could be incorporated into potent inhibitors.

In a preliminary effort to gain insight into hMetAP-2's binding pocket and especially to explore enantiomeric

Keywords: Methionine aminopeptidase; X-ray crystallography; Enantiomer discrimination; π-Cation interaction; D-Methionine; L-Methionine.
* Corresponding author at present address: Department of Biological Chemistry and Molecular Pharmacology, Harvard Medical School, 240 Longwood Avenue, C-643, Boston, MA 02115, USA. Tel.: +1 617 432 2845; fax: +1 617 432 3702; e-mail: jon_clardy@hms.harvard.edu

0960-894X/$ - see front matter © 2006 Elsevier Ltd. All rights reserved.
doi:10.1016/j.bmcl.2006.02.047

inhibitor binding, we carried out high-resolution crystal structure determinations for MetAP-2 in complex with L- and D-methionine at 1.9 and 2.0 Å resolution, respectively. Recombinant hMetAP-2 was expressed and purified as previously reported[13] and crystals of hMetAp-2 could be grown in two days at 4 °C using the sitting drop vapor diffusion technique.[14] Lack of reproducibility in preparing hMetAP-2 crystals under the original crystallization conditions prompted us to investigate the protein's stability. N-Terminal amino acid sequence analysis was performed at the BioResource Center at Cornell University using pre-formed hMetAP-2 crystals[15] indicating that a fragment of hMetAP-2 starting at residue Gly108 is the only detectable species in our crystals. The crystallization of this stable truncated hMetAP-2 fragment of approximately 42 kDa is consistent with the results recently reported by Yang et al.[16] In their work, analysis of full-length and truncated hMetAP-2 shows that the deletion of the 107 N-terminal residues from hMetAP-2 does not affect the overall structure of the peptidase domain and does not alter its kinetic behavior or the binding affinities of inhibitors.

Crystals of the L-Met and D-Met complexes were obtained by soaking native hMetAP-2 crystals with saturated solutions of the tripeptide L-Met-L-Ala-L-Ser (purchased from Sigma) or D-methionine (purchased from Aldrich). Data collections for the (L-Met)MetAP-2 and (D-Met)MetAP-2 complexes were performed at the Advanced Photon Source (APS, 14-BM-C beam line) and the Cornell High Energy Synchrotron Source (CHESS, F2-beam line), respectively. Data collection statistics are shown in Table 1. Crystals of the two complexes proved to be isomorphous to those previously obtained and the coordinates of the native hMetAP-2, without metals, waters or *tert*-butanol, were used to obtain an initial set of phases. L-Methionine and D-methionine molecules were clearly present in the active site, as observed by σ_A-weighted $2F_o - F_c$ and $F_o - F_c$ maps for the corresponding complexes (Fig. 1). The models were

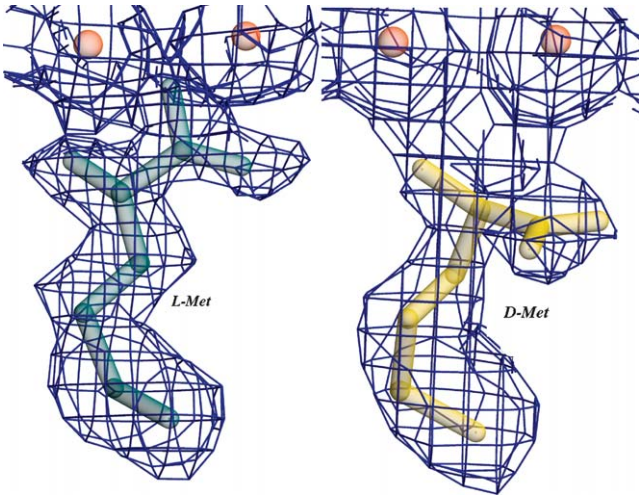

Figure 1. σ_A-weighted $2F_o - F_c$ electron density maps at 1.2σ (where σ is the root mean square value of the electron density) for L-methione (1.9 Å resolution) and D-methionine (2.0 Å resolution).

initially refined by rigid body refinement, followed by several rounds of adjusting side chain rotamers for residues using O,[17] interspersed with torsion angle simulated annealing using CNS,[18] and positional and individual *B*-factor refinement using REFMAC5[19] (Table 1).

The final model of (L-Met)hMetAP-2 complex (accession code 1KQ9) contains one protein molecule comprising residues 112–478, with two disordered regions from residues 114–115 and 139–154, plus two metal ions, a *tert*-butanol molecule, a L-methionine molecule, and 221 solvent sites treated as water oxygens. The average *B*-factors for the main chain and side chains are 26.3 and 28.7 Å^2, respectively.

L-Methionine binds in the active site, a deep hydrophobic pocket adjacent to the metal sites, through a number of different interactions (Fig. 2). One oxygen

Table 1. Crystallographic data

Data collection						
Ligand	Cell parameters (Å)	Resolution (Å)	Unique reflections	Completeness (%)	Multiplicity	R_{sym}[a] (%)
L-Met	$a = 90.7$, $b = 98.7$, $c = 101.4$	50.0–1.9	33,600	94.0	3.4	4.2
D-Met	$a = 89.8$, $b = 98.9$, $c = 100.6$	50.0–2.0	30,241	98.7	5.0	7.7

Refinement statistics									
Data set	Resolution (Å)	R_{factor}[b] (%)	R_{free}[c] (%)	RMS bond[d]		Ramachandran plot statistics regions[e]			
				Lengths (Å)	Angles (°)	Most favored (%)	Additional allowed (%)	Generously allowed (%)	Unallowed (%)
L-Met	50.0–1.9	18.1	20.9	0.07	1.88	92.3	7.0	0.3	0.3
D-Met	50.0–2.0	19.1	21.8	0.09	1.41	92.8	6.6	0.3	0.3

L-Met and D-Met raw data were merged and scaled using DENZO and SCALEPACK.[21]

[a] $R_{sym} = \sum|I_0 - \langle I\rangle|/\sum I_0$, where $\langle I\rangle$, average intensity obtained from multiple observations of symmetry related reflections.

[b] $R_{factor} = \sum|F_o - F_c|/\sum F_o$, where F_o and F_c are the observed and calculated structure factor amplitudes, respectively.

[c] R_{free} = *R* factor calculated from 5% of the data chosen randomly and omitted during refinement.

[d] Root mean square deviation from ideal geometry and root mean square variation in the *B* factors of bonded atoms.

[e] Ramachandran plot statistics were calculated using PROCHECK.[20]

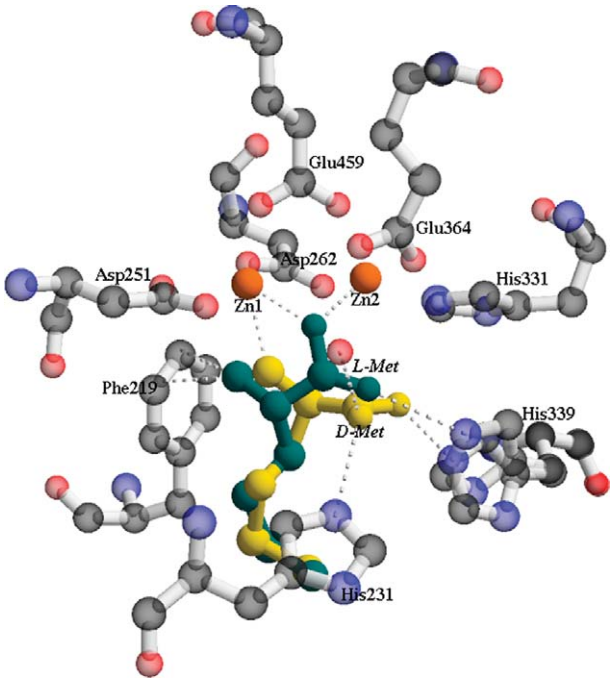

Figure 2. Three-dimensional representation of the hMetAP-2 active site showing the superimposition of L- and D-Met complexes.

of the carboxylate bridges the two metal centers, while the other oxygen is hydrogen bonded to the imidazole of conserved His339 (3.25 Å) and two water molecules (2.95 and 2.97 Å, Fig. 2). In the (L-Met)hMetAP-2 complex, the amino group of the methionine interacts with the edge of the π-electron cloud of Phe219. The distance between the N-terminal nitrogen of L-Met (N^{Met}) and CZ is 3.0 Å, N^{Met}-Cε1 is 3.68 Å, and N^{Met}-Cε2 is 2.86 Å, and this interaction will be addressed shortly. This location relative to Phe219 places the nitrogen 2.38 Å from metal site 1.

The side chain of L-Met is accommodated in a hydrophobic tunnel defined by Phe219, Gly222, Ile338, Met384, and Ala414. The closest distance observed between L-Met and residues that comprise the active site is 3.6 Å between Sδ of L-Met and Cβ of Ala414. There is no significant movement of the residues comprising the hydrophobic pocket upon L-Met binding, which recapitulates the lack of reorganization seen on fumagillin binding,[13] and suggests that the binding pocket is preorganized for binding a methionine side chain.

The final model of (D-Met)hMetAP-2 complex (accession code 1KQ0) contains one protein molecule comprising residues 111–478, with a disordered loop comprising residues 139–154, two metal ions, a *tert*-butanol molecule, a D-Met and 192 solvent sites treated as water oxygens. The average *B*-factors for the main chain and side chains are 27.4 and 27.5 $Å^2$, respectively.

The side chain of D-methionine is located in the same hydrophobic pocket as L-methionine's and makes the same hydrophobic interactions. In particular, the closest distances observed between L-Met and residues comprising the hydrophobic pocket are 3.79 Å for Sδ of L-Met ($Sδ^{Met}$) and Cβ of Phe219, and 3.94 Å for $Sδ^{Met}$ and Cβ of Ala414.

The carboxyl, amino, and α-hydrogen of D-methionine must reorient relative to their locations in the L-methionine complex to accommodate the change in absolute stereochemistry (Fig. 2). The carboxylate is roughly in the same location but with a different orientation, and the amino and α-hydrogen switch places (Fig. 2). The plane of the carboxylate group rotates roughly 90° while maintaining an interaction with His339 (2.17 Å). New interactions with the conserved His231 (3.04 Å) and a water molecule (2.76 Å) complete the interactions of the carboxylate, which does not interact with the metal sites in the D-Met complex. The amino group occupies a new location with no π-cation interaction to Phe219, a hydrogen bond to the side chain of Asp251 (3.02 Å), and a closer approach to the metals.

It has long been accepted that multiple noncovalent interactions such as hydrogen bonds, salt bridges, and hydrophobic contacts play an important role in stabilizing protein folding and protein–ligand interactions. More recently, π-cation interactions have also been shown to contribute to folding, stability of biological systems, and molecular recognition process.[22–26] Burley and Petsko have thoroughly documented the preference of a protonated amino group to interact with the center of the π-electron cloud of an aromatic ring.[24] More recently, Zaric et al. proposed a variation on this interaction, the metal ligand aromatic cation-π interaction (MLACπ), in metalloproteins.[25] In MLACπ interactions, the metal interacts with the lone pair of an unprotonated amino group to mimic a protonated amino group, which then interacts with the π-electrons of an aromatic ring. Because of geometrical constraints and the lack of a fully protonated amino group, the interaction is often to the side, not the center, of the ring.

The (L-Met)hMetAP-2 crystal structure indicates a MLACπ interaction between the amino group of methionine and Phe219. Phe219, the aromatic ring identified to take part of MLACπ in (L-Met)hMeTAP-2, is conserved in all type 2 MetAPs but not in type I MetAPs, where Phe219 is replaced by a conserved Lys residue.

Interestingly, a comparison among the three-dimensional structures of other members of the aminopeptidase family suggests that weak interactions such as hydrogen bonds, π-cation, and others may be required for proper recognition and positioning of their natural substrate. For example, the structure of the (L-Met)eMetAP-1 complex reveals that besides the N-terminal interaction to metal site 2 previously described, a threonine residue was found to interact with the amino nitrogen of the substrate (2.95 Å, 30). Aminopeptidase P from *E. coli* (eAMPP) is a proline peptidase that specifically releases the N-terminal residue from a peptide where the next residue is a proline.[27] As observed in MetAPs, AMPP is activated in the presence of divalent metal ions coordinating with the same conserved residues. A superposition between eAMPP and hMetAP-2 reveals that

Phe219 is replaced by Tyr219, allowing hydrogen bond formation with the N-terminal nitrogen from the substrate.

In summary, the present work reveals the binding modes of the reaction product, L-methionine and its enantiomer D-methionine, determined by X-ray crystallography at 1.9 and 2.0 Å, respectively. These results suggest that different absolute configurations can be accommodated in the active site and that structure-based inhibitors exploiting both binding modes could be considered.

Acknowledgments

This work was supported in part by Fundação de Amparo a Pesquisa do Estado de São Paulo (to M.C.N.) and National Institute of Health Grant CA59021 (to J.C).

References and notes

1. Ben-Bassat, A.; Bauer, K.; Chang, S. Y.; Myambo, K.; Boosman, A.; Chang, S. *J. Bacteriol.* **1987**, *169*, 751.
2. Bradshaw, R. A.; Brickey, W. W.; Walker, K. W. *Trends Biochem. Sci.* **1998**, *23*, 263.
3. Kendall, R. L.; Yamada, R.; Bradshaw, R. A. *Methods Enzymol.* **1990**, *185*, 398.
4. Chang, S. Y. P.; McGary, E. C.; Chang, S. *J. Bacteriol.* **1989**, *171*, 4071.
5. Li, X.; Chang, Y.-H. *Proc. Natl. Acad. Sci. U.S.A.* **1995**, *92*, 12357.
6. Griffith, E. C.; Su, Z.; Turk, B. E.; Chen, S.; Chang, Y.; Wu, Z.; Biemann, K.; Liu, J. O. *Chem. Biol.* **1997**, *4*, 461.
7. Sin, N. Y.; Meng, L.; Wang, M. Q. W.; Wen, J. J.; Bornmann, W. G.; Crews, C. M. *Proc. Natl. Acad. Sci. U.S.A.* **1997**, *94*, 6099.
8. Ingber, D.; Fujita, T.; Kishimoto, S.; Sudo, K.; Kanamaru, T.; Brem, H.; Folkman, J. *Nature* **1990**, *348*, 555.
9. Folkman, J. *J. Natl. Cancer* **1990**, *82*, 4.
10. Folkman, J.; Watson, K.; Ingber, D.; Hanahan, D. *Nature* **1989**, *339*, 58.
11. Folkman, J.; Ingber, D. E. *Ann. Surg.* **1987**, *206*, 374.
12. Lowther, W. T.; Orville, A. M.; Madden, D. T.; Lim, S.; Rich, D. H.; Mathews, B. W. *Biochemistry* **1999**, *38*, 7678.
13. Liu, S.; Widom, J.; Kemp, C. W.; Crews, C. M.; Clardy, J. *Science* **1998**, *282*, 1324.
14. Protein was dialyzed against 10 mM HEPES (pH 7.4), 100 mM NaCl and 10% glycerol and concentrated up to 25 mg/ml. The reservoir solution contained 18–23% *tert*-butanol in 70 mM sodium citrate buffer, pH 5.3–5.6. hMetAP-2 crystals were cross-linked using 0.07% glutaraldehyde and incubated with a 12 mM zinc acetate solution for 24 h.
15. Amino acid sequence analysis of hMetAP-2 was performed by gently transferring and washing several hMetAP-2 crystals into a fresh protein-free crystallization solution. The crystals were dissolved in 2× SDS–PAGE gel-loading buffer, run on a 10% gel, and the single band was transferred onto Immobilon-P membrane (Millipore).
16. Yang, G.; Kirkpatrick, R. B.; Ho, T.; Zhang, G. F.; Liang, P. H.; Johanson, K. O.; Casper, D. J.; Doyle, M. L.; Marino, J. P.; Thompson, S. K.; Chen, W. F.; Tew, D. G.; Meek, T. D. *Biochemistry* **2001**, *35*, 10645.
17. Jones, T. A.; Zou, J. Y.; Cowan, S. W.; Kjeldgaard, M. *Acta Crystallogr.* **1991**, *A47*, 110.
18. Brunger, A. T.; Adams, P. D.; Clore, G. M.; DeLano, W. L.; Gros, P.; Grosse-Kunstleve, R. W.; Jiang, J. S.; Kuszewski, J.; Nilges, M.; Pannu, N. S.; Read, R. J.; Rice, L. M.; Simonson, T.; Warren, G. L. *Acta Crystallogr.* **1998**, *D54*, 905.
19. Murshudov, G. N.; Vagin, A. A.; Dodson, E. J. *Acta Crystallogr.* **1997**, *D53*, 240.
20. Laskowski, R. A.; MacArthur, M. W.; Moss, D. S.; Thornton, J. M. *J. Appl. Crystallogr.* **1993**, *26*, 283.
21. Otwinowski, Z., 'Oscilation Data Reduction Program'. In *Proceedings of the CCP4 Study Weekend: Data Collection and Processing*, January 29–30 1993. Compiled by: Sawyer, L., Isaacs, N., Bailey, S. SERC Daresbury Laboratory, England, pp 56–62.
22. Gallivan, J. P.; Dougherty, D. A. *Proc. Natl. Acad. Sci. U.S.A.* **1999**, *96*, 9459.
23. Ma, J. C.; Dougherty, D. A. *Chem. Rev.* **1997**, *97*, 1303.
24. Burley, S. K.; Petsko, G. A. *FEBS Lett.* **1986**, *203*, 139.
25. Zaric, S. D.; Popovic, D. M.; Knapp, E. *Chem. Eur. J.* **2000**, *21*, 3935.
26. Dougherty, D. A. *Science* **1996**, *271*, 163.
27. Wilce, M. C.; Bond, C. S.; Dixon, N. E.; Freeman, H. C.; Guss, J. M.; Lilley, P. E.; Wilce, J. A. *Proc. Natl. Acad. Sci. U.S.A.* **1998**, *95*, 3472.